journal

J. Am. Ceram. Soc., 94 [1] 145–150 (2011)
DOI: 10.1111/j.1551-2916.2010.04053.x

Liquid–Liquid Phase Separation in Photo-Thermo-Refractive Glass

Guilherme P. Souza,[†,‡] Vladimir M. Fokin,[‡] Camila F. Rodrigues,[‡] Ana Candida M. Rodrigues,[‡] Edgar D. Zanotto,[‡] Julien Lumeau,[§] Larissa Glebova,[§] and Leonid B. Glebov[§]

[‡]Universidade Federal de São Carlos, DEMa/LaMaV—Vitreous Materials Laboratory, São Carlos, São Paulo 13565-905, Brazil

[§]CREOL, The College of Optics and Photonics, University of Central Florida, Orlando, Florida 32816-2700

Photo-thermo-refractive (PTR) glass is an optical Na–Al–Zn–K–O–F–Br silicate glass doped with Ag, Ce, Sb, and Sn that undergoes photo-thermo-induced volume crystallization of nano-sized NaF responsible for localized refractive index changes. PTR glass has found numerous commercial applications, but the intricate mechanism of photo-thermo crystallization is far from being understood. In this paper, we demonstrate that, additional to crystalline phase precipitation, liquid–liquid phase separation (LLPS), i.e. amorphous droplets embedded in the matrix glass, appears concurrently over a wide range of temperatures. The immiscibility temperature is 925°C. The droplet phase is richer in SiO_2, rendering the alkali-rich remaining matrix glass a lower glass transition temperature and a higher electrical conductivity than the original glass. The droplet's surface does not catalyze NaF nucleation. Although the effects of LLPS on optical properties of PTR glass are still to be explored, it could contribute to unwanted scattering losses and/or uncontrolled refractive index change. The substantial change in the original glass composition resulting from LLPS should play an important role on NaF crystallization kinetics, and therefore must be considered for an overall understanding of the crystallization mechanism underpinning the refractive index change in PTR glass.

I. Introduction

PHOTO-THERMO-REFRACTIVE (PTR) glass is an optical Na_2O–Al_2O_3–ZnO–K_2O silicate glass containing Br and F and doped with Ce, Ag, Sb, and Sn. This glass is photosensitive in the near-UV region and allows for producing a local refractive index change after UV illumination and subsequent thermal treatment above the glass transition temperature. To a first approximation, the primary photo-thermo-induced reactions in PTR glass are[1]: (i) photo-oxidation of Ce^{3+} and formation of atomic silver during exposure to UV ($Ag^{+}+Ce^{3+}+h\nu \rightarrow Ag^{0}+Ce^{4+}$), (ii) atomic silver clustering during a first thermal treatment at 450°–500°C, and (iii) heterogeneous nucleation and growth of NaF nanocrystals on further heating at a higher temperature. It has been shown that unexposed PTR glass also undergoes NaF crystallization (to a lesser degree),[2] but Br-free glass does not show signs of NaF volume crystallization.[3] Therefore, the actual mechanism of photo-thermo-induced crystallization is more complex than the above described scheme. Despite the fact that the detailed mechanism and kinetics of crystallization of PTR glass are unknown, high-efficiency volume diffractive optical elements (DOE) are being fabricated in PTR glass using the knowledge that different extents of crystalline phase precipitation result in a difference between refractive indices in UV-exposed and unexposed areas of the glass.[4] DOE in PTR glass have numerous applications, such as narrow band spectral and angular filters, laser beam deflectors, splitters, and attenuators.[5]

Liquid–liquid phase separation (LLPS) is a common phenomenon in multicomponent oxide glasses. Because metastable LLPS in glass occurs at temperatures below the liquidus, even at relatively high viscosities, the newly formed glassy phases develop inhomogeneous structures consisting of either interconnected phases or isolated rounded regions embedded in a continuous matrix glass (the so-called droplet structure). The type of micro- or nanostructure formed depends on the composition of the original glass and temperature and dwell time of thermal treatment. Keen interest in the problem of LLPS, emerged in the 1960 and 1970, resulted in multiple publications and a number of monographs on the theme.[6,7]

In spite of the long history of investigation of PTR glass and its notable optical applications, the problem of LLPS has never been addressed in this glass, and therefore not yet considered in the commonly accepted scheme of crystallization. On the other hand, it has been shown that LLPS plays a very important role on the dopant-assisted crystallization of photochromic glasses.[8] Therefore, the present paper aims at addressing the problem of LLPS in PTR glass.

II. Experimental Procedure

A PTR glass with composition $15Na_2O$–$5ZnO$–$4Al_2O_3$–$70SiO_2$–$5NaF$–$1KBr$–$0.01Ag_2O$–$0.01CeO$–$0.01SnO_2$–$0.03Sb_2O_3$ (mol%) was prepared via melting at 1460°C and annealing at 460°C for 1 h, followed by cooling to room temperature at 0.1 K/min. The glass was not UV exposed. For isothermal treatments, glass samples not larger than $3 \times 3 \times 3$ mm^3 aged at room temperature were dropped into a box furnace stabilized previously at certain temperatures ranging from 520° to 930°C. After a given period of time, samples were quenched to room temperature in air, or more severely, in a mixture of ice and water. In both cases, the cooling rates of the quenching experiments are estimated to exceed 500 K/min. X-ray diffraction (XRD) measurements were carried out on powdered samples using a Siemens D5005 (Siemens, Munich, Germany) XRD operating at 40 mA and 40 kV. Cu$K\alpha$ (1.5406 Å) was used as the incident radiation to scan samples from $20^\circ \leq 2\theta \leq 60^\circ$ at a scanning speed of 0.6°/min. To investigate the microstructure of the samples after heat treatments, a combination of chemical etching and optical microscopy and scanning electron microscopy (SEM) was used. From chipped glass resulting from sample cracking during quenching in the water–ice mix, flat chips were selected for etching with hydrofluoric acid (HF). The etched chips were placed on to a glass slide for optical microscopy. A Leica DMRX optical microscope coupled with a Leica (Leica,

L. Pinckney—contributing editor

Manuscript No. 27950. Received May 1, 2010; approved July 4, 2010.
This work was supported by DARPA ADHELS program, contract HR-0011-06-1-0010.
[†]Author to whom correspondence should be addressed. e-mail: gparente003@hotmail.com

Wetzlar, Germany) DFC490 CCD camera was used in the reflected light mode. A Philips (Philips, Amsterdam, the Netherlands) XL30 TMP SEM was used for secondary electron (SE) imaging of etched samples. Sample preparation for SEM was very similar to that for optical microscopy, but involved additional steps such as fixing on an aluminum stub using double-sided carbon tape, and coating with a thin layer of gold. A Netzsch 404 differential scanning calorimeter (DSC) (Netzsch, Selb/Bavaria, Germany) was used to measure the T_g of original as well as heat-treated glass samples, which were run in a platinum crucible at 10 K/min from room temperature until 650°C.

The chemical compositions of glassy phases resulted from LLPS differ from that of a parent glass. To probe such a compositional change, electrical conductivity measurements using impedance spectroscopy were carried out in both liquid-phase-separated and untreated (original) glass samples, which were ground and polished. Platinum-sputtered electrodes were deposited on both parallel faces. Measurements were conducted, on heating, at temperatures between 250° and 470°C in a box furnace, using a Solartron 1260 impedance analyzer (Solartron Instruments, Hampshire, U.K.). Alternating current at a variable frequency range from 1 Hz to 10 MHz was used. Impedance data represented in the complex plane plot produce a semicircle followed by a spike due to electrode polarization, characteristic of ionic conduction.[9] Resistance (R) can be measured at a given temperature by taking the intercept of the semicircle with the real part of the impedance axis, at low frequencies. Electrical conductivity (σ) is then calculated as

$$\sigma = \frac{L}{R \cdot S} \tag{1}$$

where L is the sample's thickness, and S is the electrode's area.

III. Results

(1) XRD and SEM

An XRD trace of PTR glass heat treated at 760°C for 15 min is shown in Fig. 1(a). This temperature was chosen because, according to Fokin *et al.*[10] the PTR glass melt is undersaturated in NaF at temperatures above 745°C, and therefore, NaF crystals cannot form at such temperatures. This is confirmed by the absence of crystalline NaF peaks in the XRD spectrum. However, it is clear from Fig. 1(b) that the glass develops distinctive opalescence after such heat treatment. The SEM/SE images shown in Figs. 2(a)–(b) are for the same sample (heat treated at 760°C for 15 min), but after etching of a fractured surface. A droplet-like structure, similar to that first reported by Souza *et al.*[11] in PTR glass, is evident. Because XRD shows no crystalline peaks (Fig. 1(a)) apart from a very small bump at ~42.5° 2θ likely to be due to negligible volume fraction of residual NaBr,[11] one can infer that the original glass has separated into two distinct glassy phases—droplets and continuous matrix glass. It is worth pointing out that no structure was revealed in the untreated glass (i.e., from the initial melting and annealing) after etching with HF and optical and SEM analysis. Such kind of droplet-like structure is typical in cases where the relative volume of one of the coexisting amorphous phases is <25%.[6] The volume fraction of the droplet phase decreases dramatically as it becomes less numerous after further heat treatment at 910°C for 30 min (Fig. 2(c)). A similar structure forms if a sample of original glass is heat treated directly at 910°C for 30 min (Fig. 2(e)). This fact gives indirect evidence that the microstructure shown in Figs. 2(c) and (e) indeed corresponds to an equilibrium between the two coexisting glassy phases, and that the glass does not show thermal memory regarding LLPS. The droplet structure completely disappears at 930°C (Fig. 2(d)) in the case of preliminary induced LLPS, and does not form if the original glass is directly dropped into the furnace at 930°C (Fig. 2(f)). Thus, one can conclude that the binodal temperature for the PTR glass of studied composition lies between 910° and 930°C.

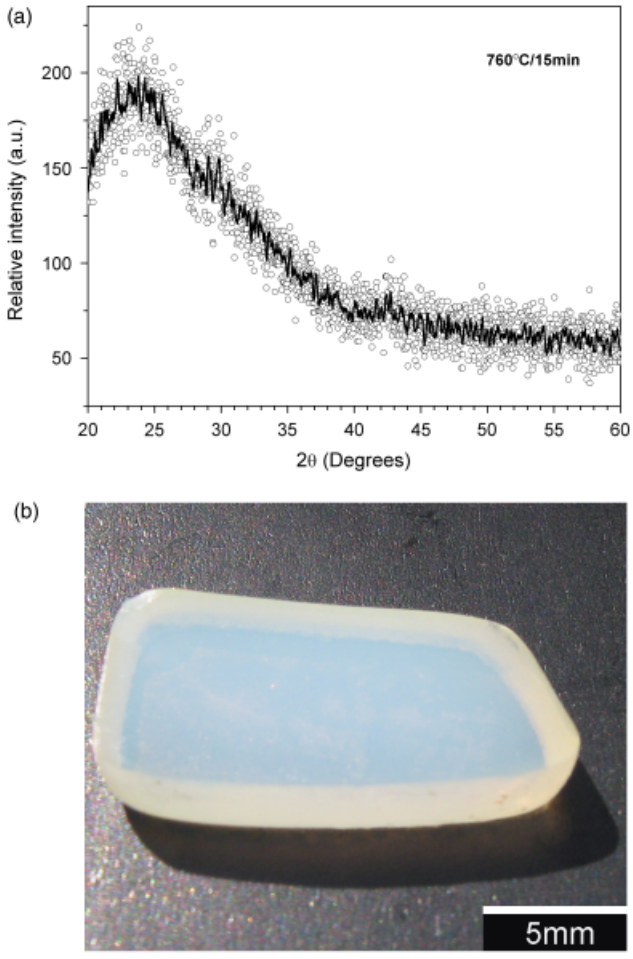

Fig. 1. (a) XRD trace of photo-thermo-refractive glass heat treated at 760°C for 15 min. Smoothing of raw data is represented by a solid line. (b) Photograph of the glass after the same thermal treatment showing clear evidence of opalescence.

(2) Optical Microscopy

Despite the fact that optical microscopy cannot fully resolve the actual shape and size of the droplet-like structure, optical micrographs presented in Fig. 3 clearly reveal the systematic decrease in the number of droplets as the temperature is increased. While the droplet structure can still be observed after heat treating at 920°C, a heat treatment at 928°C does not lead to droplet formation. Moreover, the LLPS structure preliminary induced at 760°C disappears at 928°C. Hence, we expect that the binodal temperature is about 925°C. It should be recalled that all samples in Figs. 2 and 3 were quenched in a water–ice mix. This procedure led to significant cracking. Because small pieces of broken glass with irregular shapes were used for optical microscopy, only some regions of such specimens are in focus in Fig. 3.

(3) Electrical Conductivity

The electrical conductivity of an alkali silicate glass depends on the concentration of charge carriers. In PTR glass, the main charge carrier is Na^+, because the concentrations of F^-, K^+, and Br^- are significantly smaller than that of sodium. The electrical conductivity of untreated PTR glass, and that of samples heat treated at 760°C for 15 min, are shown in Fig. 4 as a function of temperature. For a given temperature in the range of 250°–450°C, the glass heat treated at 760°C for 15 min shows higher electrical conductivity than the untreated glass. Although the observed difference in electrical conductivity is small, it was

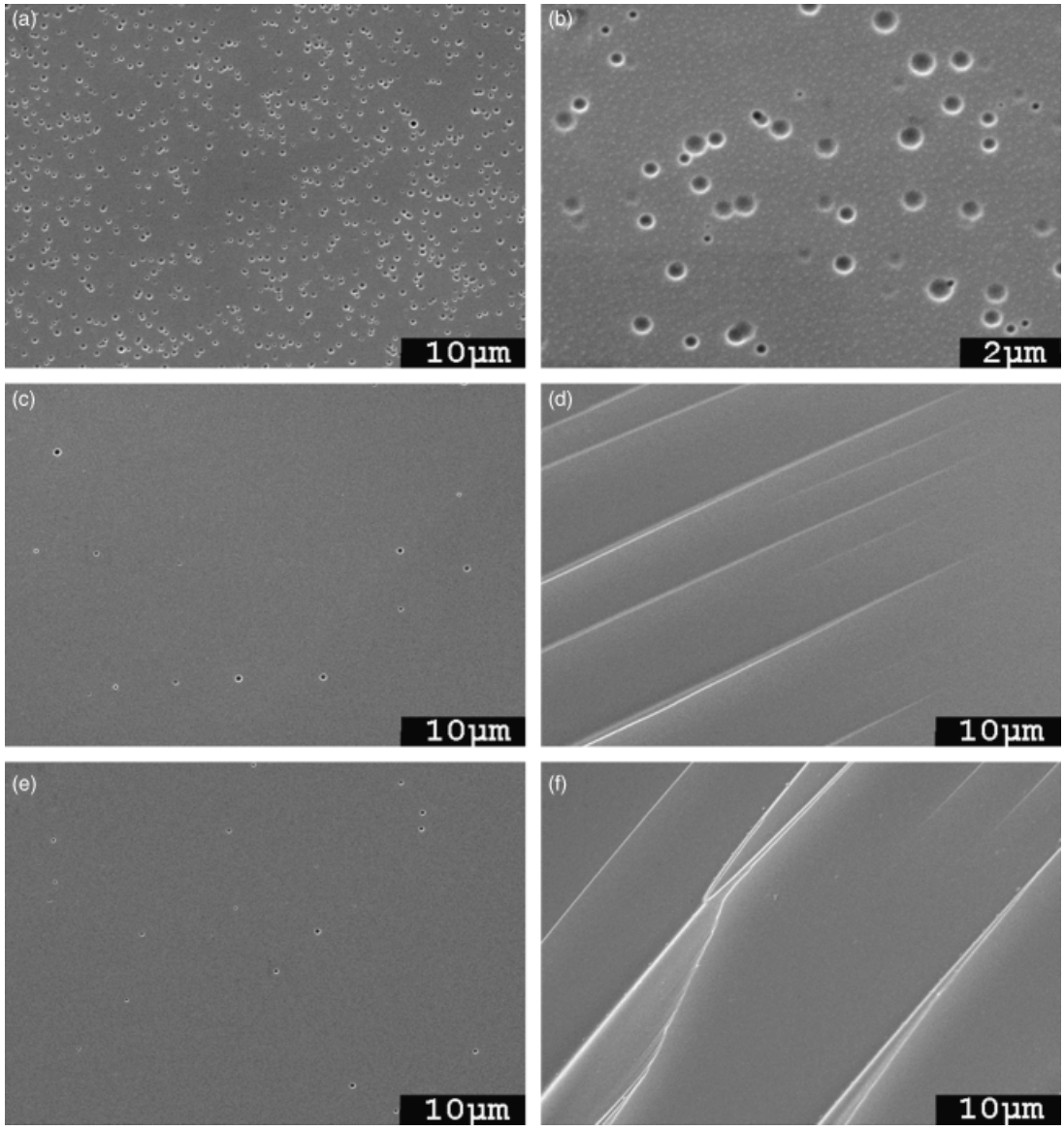

Fig. 2. SEM/SE images of photo-thermo-refractive glass heat treated at different temperatures for different periods (T, °C/t, min), quenched to room temperature, and etched in hydrofluoric acid. (a) 760°C/15 min; (b) 760°C/15 min; (c) 760°C/15 min+910°C/30 min; (d) 760°C/15 min+930°C/30 min; (e) 910°C/30 min; and (f) 930°C/30 min.

confirmed by three series of measurements, each one performed during a different heating cycle. The straight lines correspond to the linear regression of the collected experimental data, with correlation coefficients better than 0.997 and standard error lower than 5%. The activation energy for conduction is the same, within the experimental error, for both untreated (0.83 ± 0.01 eV) and heat treated (0.82 ± 0.01 eV) glass samples.

IV. Discussion

Heat treatments at temperatures higher than 760°C and lower than 925°C were shown to result in the separation of initially homogeneous parent PTR glass into two glassy phases. The droplet-like structure is typical of liquid immiscibility within the metastable region between the spinodal and binodal. Because the main components of PTR glass are Na_2O (15 mol%) and SiO_2 (70 mol%), enrichment of the matrix glass by sodium and fluorine can be expected due to formation of the droplet phase enriched by silicon oxide, as documented in the literature for the Na_2O–SiO_2 system.[6,12] Because we used etched fractured surfaces to look at the morphology of the samples with LLPS, the more HF-resistant, SiO_2-rich droplet phase was mostly pulled out of the microscopy specimen's surface, leaving traceable droplet-like cavities. It is well known that SiO_2 decreases the etching rate of the glass.[13] Chemical gradient at the interface between droplet and matrix, such as the expected (local) increase in Na, add up to the complexity of the microstructural observation and may boost droplet removal by weakening the mechanical coupling at the interface. Moreover, even during the fracturing of the sample, some droplets, having physical–mechanical properties different from the matrix glass, can be pulled out to relieve residual stresses. These difficulties hindered direct chemical analysis of the droplet with respect to matrix phase, and propped our efforts to investigate the LLPS using a nonconventional approach.

If the minor components are neglected from the original glass composition, a rough approximation in terms of sodium and silicon oxides is 17.6 mol% Na_2O and 82.4 mol% SiO_2, which lies within the field of LLPS for the Na_2O–SiO_2 system.[12] Because the main ionic conductors are Na^+ and F^- (but the concentration of fluorine is significantly smaller than that of sodium), the conductivity of the matrix glass is expected to be higher than that of the original, homogeneous glass. Indeed, Fig. 4 demonstrates a weak, but statistically well-defined increase in the conductivity of the glass after heat treatment at

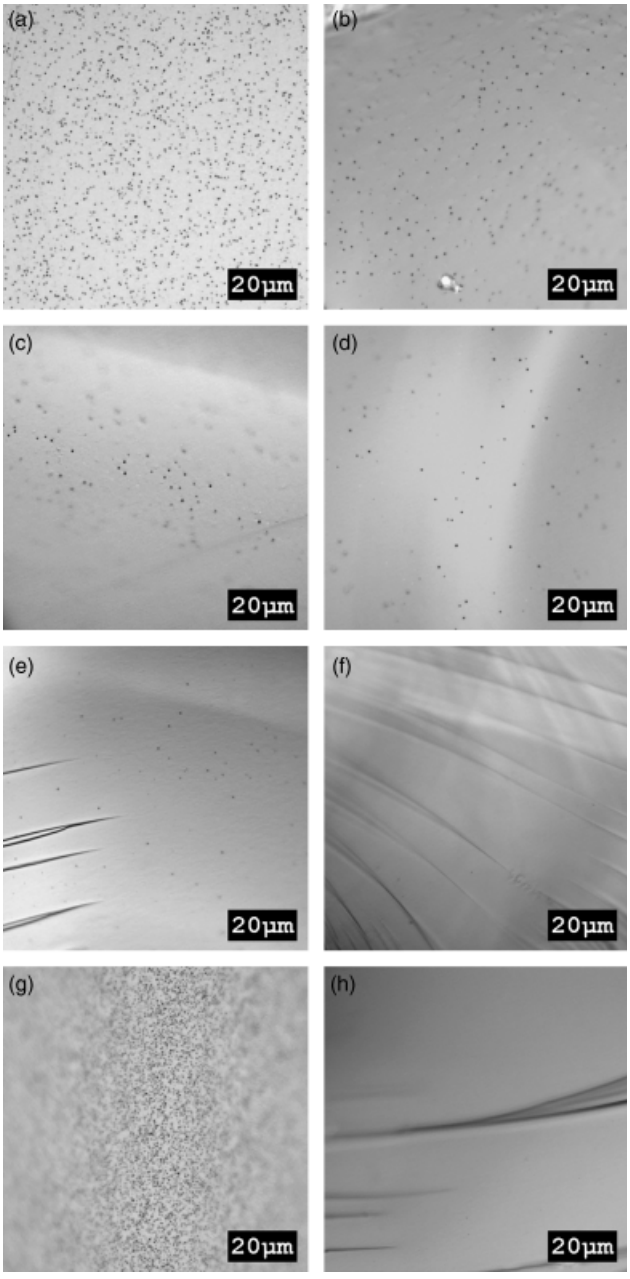

Fig. 3. Optical micrographs of photo-thermo-refractive glass heat treated at different temperatures for different periods (T, °C/t, min), quenched to room temperature, and etched in hydrofluoric acid. (a) 810°C/30 min; (b) 890°C/30 min; (c) 900°C/30 min; (d) 910°C/30 min; (e) 920°C/30 min; (f) 928°C/30 min; (g) 760°C/15 min; (h) and 760°C/15 min+928°C/30 min.

760°C for 15 min (i.e., glass sample with LLPS). This result corroborates the expected enrichment of the matrix glass by charge carriers. The volume fraction of the droplet phase formed in such sample is about 7 vol% (see Fig. 2(a)), which may be slightly overestimated had some over-etching occurred. Supposing that the droplet composition is close to SiO_2, one could expect that the Na_2O content in the matrix phase exceeds that of the original glass by no more than ~8 mol%. According to Fig. 5, which shows the conductivity of sodium silicate glass at 650 K versus SiO_2 content,[14] such evolution of glass composition (within the compositional range detailed by the double ended arrow in Fig. 5) cannot cause a strong variation of electrical conductivity. Although the above estimate is rough, it gives a reasonable idea on the extent of conductivity increase expected due to LLPS. The conductivity increase observed in PTR glass after LLPS was about 30% (Fig. 4), in line with the

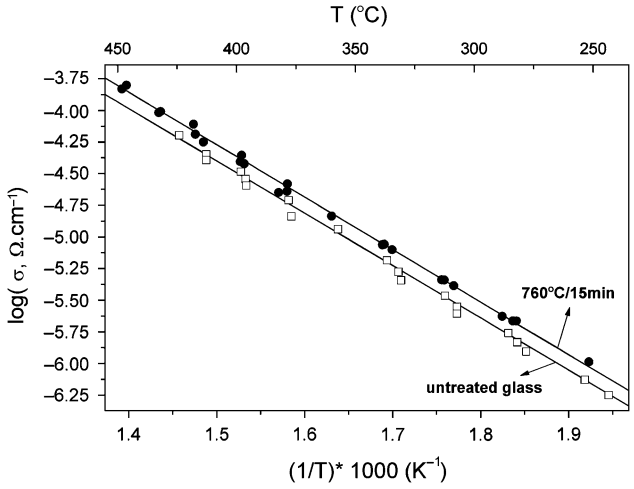

Fig. 4. Electrical conductivity as a function of temperature of photo-thermo-refractive glass untreated and heat treated at 760°C/15 min.

model Na_2O–SiO_2 system mentioned above. The approximation used for explaining the electrical conductivity data, on the basis of increase in the sodium content in the matrix glass upon LLPS to be playing a major role, can be further supported by the fact that the conductivity of sodium silicate glasses is largely unchanged by the addition of fluorine.[15]

The difference in composition between the matrix glass after liquid-phase-separation and the original glass, inferred by impedance spectroscopy measurement, is corroborated by a corresponding change in the glass transition temperature. Figure 6 presents DSC traces for original (untreated) and heat-treated glass samples. The value of T_g measured for the liquid-phase-separated glass is lower than that for the original glass. This result gives an additional evidence for the fact that the matrix glass contains less SiO_2 than the original glass, which is also in good agreement with conductivity results shown above. The kinetic aspect of LLPS can be inferred from the $T_g \times t$ curve for PTR glass heat treated at 650°C in Fokin *et al.*,[10] where it is shown that an initial drop in T_g due to LLPS is the dominant transformation before the vigorous increase in T_g due to NaF crystallization (i.e., as the matrix glass becomes poorer in Na).

It is interesting to compare the temperature of binodal (immiscibility temperature), estimated in the present work, with that for Na_2O–SiO_2 glasses in connection with the influence of fluorine on the LLPS in binary alkali silicate glasses.

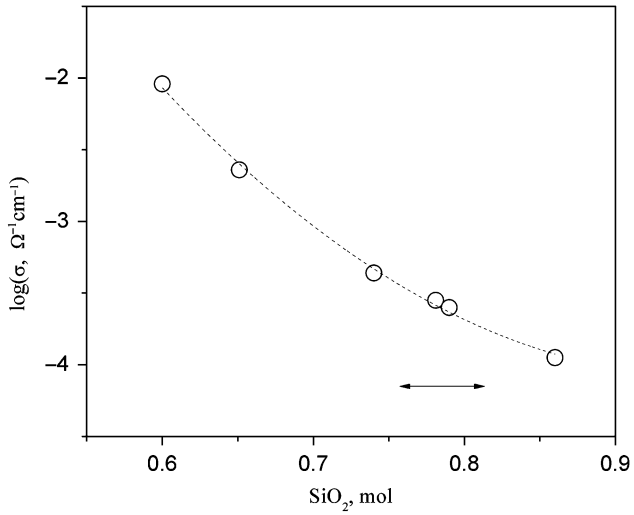

Fig. 5. Electrical conductivity as a function of SiO_2 content for Na_2O–SiO_2 glasses[14]. The expected change in composition of photo-thermo-refractive glass due to liquid–liquid phase separation is represented by a double-ended arrow.

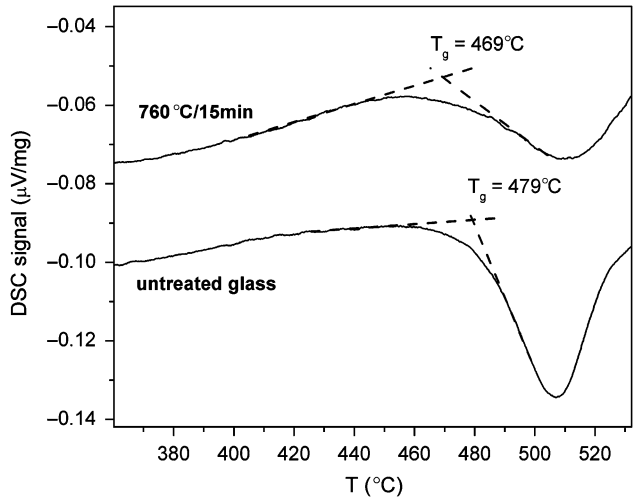

Fig. 6. DSC traces of photo-thermo-refractive glass untreated and heat treated at 760°C/15 min.

In spite of the complex composition of PTR glass, we will discuss the properties of a hypothetical glass with a composition reduced to the two main components. Such an approximation allows us to plot the temperature of the binodal (T_{bin}) together with data from Markis *et al.*[16] for glass compositions $83SiO_2 \cdot (17-x)Na_2O \cdot xNaF$ versus x (see Fig. 7). Although the reduced PTR glass composition (i.e., that which takes into account only Na_2O and SiO_2) is only an approximation, our experimental data fits the increase of immiscibility temperature with the increasing NaF content.

Up to this point, we have considered the temperature range where only LLPS occurs, i.e. above $T_{ds} = 745$°C. Here, T_{ds} ("dissolution temperature") is the temperature where the melt is saturated in NaF.[10] This means that at temperatures above T_{ds}, no NaF crystals are expected as the melt becomes under-saturated in NaF. Below T_{ds}, NaF crystallization occurs along with LLPS. Then, the question about the effect of liquid immiscibility on NaF crystallization in PTR glass becomes relevant. LLPS can induce crystallization through a change of glass composition[17–19] or via development of an interface between the liquid phases. The evolution of T_g of the matrix glass sheds some light on the kinetics of LLPS and crystallization processes, because the LLPS leads to a decrease of T_g (see e.g., Fig. 6), whereas the crystalline phase precipitation leads to an increase of T_g (due to formation of NaF crystals and consequent depletion of Na and F in the melt). As was shown in Fokin *et al.*,[10] due to the interplay between these two effects, T_g was shown to pass through a minimum (as shown by systematic T_g measurements of the samples quenched from various times during an isothermal treatment). A decrease of T_g at the first stages of heat treatment allows one to suppose that the kinetics of LLPS is faster than the overall crystallization kinetics, and because the time corresponding to the minimum of T_g is shorter, the higher the heat-treatment temperature, the difference between the kinetics of the two processes increases with the decreasing temperature.

The liquid–liquid phase-separated structure was also detected by SEM at lower temperatures, for instance at $T = 520$°C. Figure 8(a) shows the cross section of a sample heat treated at 520°C for 100 h, etched with a 2% HF solution for 1 min. Unlike the samples shown in Figs. 2 and 3, this sample was quenched in air. Because the crystals (some of them arrowed in Fig. 8(a)) have different orientations and not very clear regular morphologies, it is difficult to separate the crystals from the glassy droplet phase with similar sizes. Quantitative X-ray analysis was used in Fokin *et al.*[10] to estimate the volume fraction of crystalline NaF, which corresponds to only ~2.1 vol% in the case of the sample shown in Fig. 8(a). The XRD trace for this same sample is shown in Fig. 8(b), where the crystalline peaks correspond to NaF. Here, it should be noted that the volume fraction measured corresponds to the equilibrium volume of crystalline (NaF) phase at $T = 520$°C. Thus, it is clear that NaF crystals cannot account for all the microstructural features revealed in Fig. 8(a), because they occupy much more than 2.1 vol%, and even if one takes into account the possible effect of over-etching[20,21] of the neighboring glass. One more remark

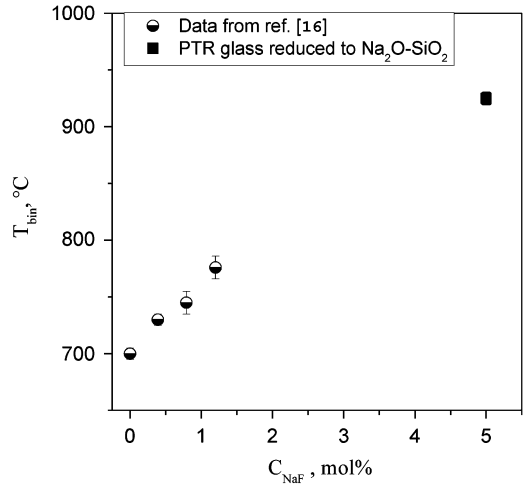

Fig. 7. Plot of the temperature of binodal (T_{bin}) for glass compositions $83SiO_2 \cdot (17-x)Na_2O \cdot xNaF$,[16] and for a hypothetical fraction of $82SiO_2 \cdot (18-x)Na_2O \cdot xNaF$ in photo-thermo-refractive glass as a function of NaF content (C_{NaF}).

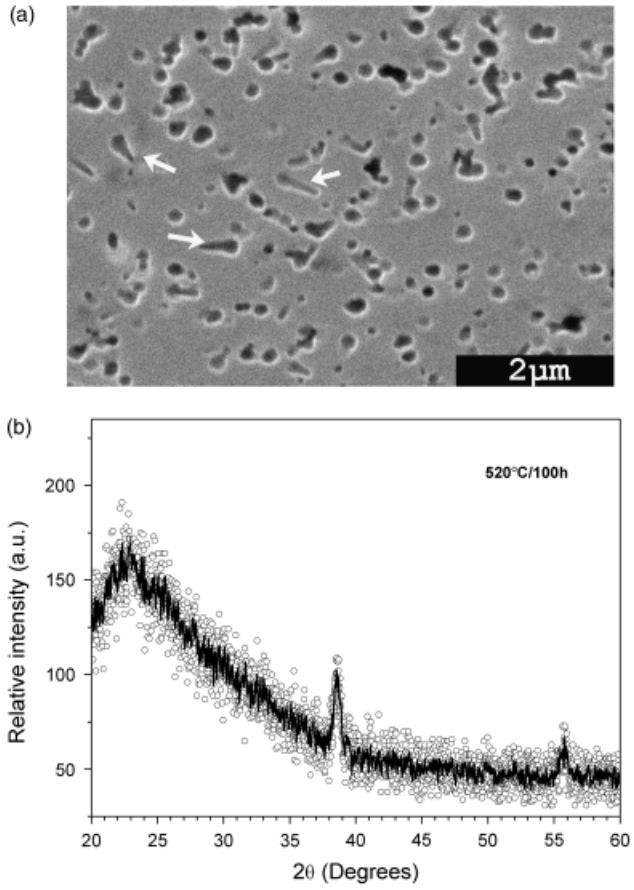

Fig. 8. SEM/SE image (a) and XRD trace (b) of photo-thermo-refractive glass heat treated at 520°C for 100 h. (b) Smoothing of raw data is represented by a solid line.

should be made regarding the microstructure shown in Fig. 8(a). NaF crystals, having the same size scale of the (amorphous) droplet phase, precipitate in the continuous matrix glass. However, nucleation of NaF crystals does not depend on the droplet phase, i.e. the droplet's surface does not catalyze NaF nucleation. This finding corroborates the earlier proposal of Zanotto and colleagues.[17–19] The matrix glass after LLPS has higher Na and F contents than the original PTR glass. Hence, we can suppose that super-saturation of the matrix glass in NaF is higher than that of the original glass. This means that LLPS might enhance NaF crystallization kinetics.

In the present study, we demonstrated that liquid immiscibility, typical for the metastable field, with a droplet structure appears in PTR glass over a wide range of temperatures. Although its effect on optical properties of PTR glass-based DOEs is still to be explored, one can expect that LLPS could contribute to scattering losses and/or refractive index changes. New compositions may be devised specifically to change the miscibility gap of this multicomponent sodium silicate system, so that optical properties can be tailored. Moreover, NaF nucleation kinetics is expected to vary if the glass composition is changed, as discussed above. This can be achieved not only via changing the glass batch composition but also via adjusting the extent of liquid immiscibility produced through controlled thermal-treatment parameters.

V. Conclusions

LLPS with a droplet structure was shown in PTR glass heat treated over a wide range of temperatures. The continuous matrix glass after LLPS has lower SiO_2 content than the droplet phase, as revealed by its higher electrical conductivity, and lower T_g compared with the original glass. The liquid immiscibility observed in PTR glass is in line with that in a model Na_2O–SiO_2 system, but phase separation was reinforced by fluorine. The droplet's surface does not catalyze NaF nucleation. This finding corroborates earlier proposed models. The currently accepted crystallization mechanism in PTR glass requires further study taking into account LLPS, as well as its implications in optical properties.

Acknowledgments

E. D. Z. and A. C. M. R. acknowledge Brazilian funding agencies CNPq and FAPESP contract 2007/08179-9. G. P. S., V. M. F., and C. F. R. acknowledge FAPESP, contracts 2008/02645-0, 2008/00475-0, and 2007/05214-8, respectively. J. L. acknowledges the IMI-NFG support under NSF grant No DMR-0844014.

References

[1]S. D. Stookey, G. H. Beall, and J. E. Pierson, "Full-Color Photosensitive Glass," *J. Appl. Phys.*, **49** [10] 5114–23 (1978).
[2]J. Lumeau, A. Sinitskii, L. Glebova, L. B. Glebov, and E. D. Zanotto, "Spontaneous and Photo-Induced Crystallization of Photo-Thermo-Refractive Glasses," *Phys. Chem. Glasses*, **48** [4] 281–4 (2007).
[3]L. Glebova, J. Lumeau, M. Klimov, E. D. Zanotto, and L. B. Glebov, "Role of Bromine on the Thermal and Optical Properties of Photo-Thermo-Refractive Glass," *J. Non-Cryst. Solids*, **354**, 456–61 (2008).
[4]V. A. Borgman, L. B. Glebov, N. V. Nikonorov, G. T. Petrovskii, V. V. Savvin, and A. D. Tsvetkov, "Photothermal Refractive Effect in Silicate Glasses," *Sov. Phys. Dokl.*, **34**, 1011–3 (1989).
[5]L. B. Glebov, "Photosensitive Holographic Glass—New Approach to Creation of High Power Lasers," *Phys. Chem. Glasses: Eur. J. Glass Sci. Technol. B*, **48**, 123–8 (2007).
[6]O. V. Mazurin and E. A. Porai-Koshits, *Phase Separation in Glass*. North-Holland, Amsterdam, the Netherlands, 1984.
[7]O. V. Mazurin, G. P. Roskova, and V. I. Averjanov, "Two-Phase Glasses: Structure, Properties, Applications"; Edited by B. G. Varshal. Nauka, Leningrad, 1991, 276 pp. (in Russian).
[8]V. A. Tsekhomskii and I. V. Tunimanova, "Photochromism and Micro-Phase-Separation"; pp. 132–4 in *Likvatsionnye Yavleniya v Steklakh*, Edited by E. A. Porai-Koshits. Nauka, Leningrad, 1969.
[9]J. R. MacDonald (ed.) *Impedance Spectroscopy*. Wiley, New York, 1987.
[10]V. M. Fokin, G. P. Souza, E. D. Zanotto, J. Lumeau, L. Glebova, and L. B. Glebov, "Sodium Fluoride Solubility and Crystallization in Photo-Thermo-Refractive Glass," *J. Am. Ceram. Soc.*, **93** [3] 716–21 (2010).
[11]G. P. Souza, V. M. Fokin, E. D. Zanotto, J. Lumeau, L. Glebova, and L. B. Glebov, "Micro and Nanostructures in Partially Crystallized Photothermorefractive Glass," *Phys. Chem. Glasses—Eur. J. Glass Sci. Technol. Part B*, **50** [5] 311–20 (2009).
[12]W. Haller, D. H. Blackburn, and J. H. Simmons, "Miscibility Gaps in Alkali-Silicate Binaries—Data and Thermodynamic Interpretation," *J. Am. Ceram. Soc.*, **57** [3] 120–6 (1974).
[13]M. Tomozawa and T. Takamori, "Effect of Phase Separation on HF etch rate of Borosilicate Glasses," *J. Am. Ceram. Soc.*, **60** [7–8] 301–4 (1981).
[14]D. Ravaine, "Conduction ionique et relaxation de conduction Dans les verres a base d'oxydes Ph.D. Thesis, Grenoble Institute of Technology, Grenoble, France, 1976
[15]A. A. Kiprianov and N. G. Karpukhina, "Oxyhalide Silicate Glasses," *Glass Phys. Chem.*, **32** [1] 1–27 (2006).
[16]J. H. Markis, K. Clemens, and M. Tomozawa, "Effect of Fluorine on the Phase Separation of Na_2O–SiO_2 Glasses," *J. Am. Ceram. Soc.*, **64** [1] C20 (1981).
[17]E. D. Zanotto, P. F. James, and A. F. Craievich, "The Effects of Amorphous Phase Separation on Crystal Nucleation Kinetics in BaO–SiO_2 Glasses. Part 3: Isothermal Treatments at 718–760°C, SAXS Results," *J. Mater. Sci.*, **21**, 3050–64 (1986).
[18]E. D. Zanotto and P. F. James, "The Compositional Dependence of Crystal Nucleation in Li_2O–SiO_2 Glasses," *Glastech. Ber.*, **56k**, 794–9 (1983).
[19]A. F. Craievich, E. E. Zanotto, and P. F. James, "Kinetics of Sub-Liquidus Phase Separation in Silicate and Borate Glasses. A Review," *Bull. Soc. Franc. Min. Crist.*, **106**, 169–84 (1983).
[20]R. A. McCurrie and R. W. Douglas, "Diffusion-Controlled Growth of 2nd Phase Particles in a Lithium-Silicate Glass," *Phys. Chem. Glasses*, **8** [4] 132–9 (1967).
[21]D. G. Burnett and R. W. Douglas, "Liquid–Liquid Phase Separation in Soda-Lime–Silica System," *Phys. Chem. Glasses*, **11** [5] 125–35 (1970). □